ELSEVIER

Materials Science and Engineering A313 (2001) 145–152

MATERIALS SCIENCE & ENGINEERING A

www.elsevier.com/locate/msea

Magnetic and X-ray diffraction measurements for the determination of retained austenite in TRIP steels

L. Zhao [a,b,*], N.H. van Dijk [c], E. Brück [d], J. Sietsma [b], S. van der Zwaag [a,b]

[a] *Netherlands Institute for Metals Research, P.O. Box 5008, Rotterdamseweg 137, GA Delft, The Netherlands*
[b] *Laboratory for Materials Science, Delft University of Technology, Rotterdamseweg 137, 2628 AL Delft, The Netherlands*
[c] *Interfaculty Reactor Institute, Delft University of Technology, Mekelweg 15, 2629 JB Delft, The Netherlands*
[d] *Van der Waals — Zeeman Institute, University of Amsterdam, Valckenierstraat 65, 1018 XE, Amsterdam, The Netherlands*

Received 6 June 2000; received in revised form 20 December 2000

Abstract

The accurate determination of the volume fraction of retained austenite is of great importance for the optimization of transformation induced plasticity (TRIP) steels. In this work, two aluminium-containing TRIP steels are studied by means of magnetization and X-ray diffraction (XRD) measurements. By fitting the field dependence of the approach to saturation in the magnetization curves, the saturation magnetization is determined, which is linearly related to the volume fraction of retained austenite. Moreover, information with respect to the microstructure can be obtained from the fitting parameters and the demagnetizing factor for the magnetization curve. The volume fractions obtained from the magnetization measurements are compared with data from XRD measurements. A discussion of the data suggests that magnetization measurements lead to more reliable results and a more sensitive detection of the retained austenite than XRD measurements.

Keywords: TRIP steels; Retained austenite; Magnetization; Microstructure

1. Introduction

The development of steels during the last decade have shown that transformation induced plasticity (TRIP) steels constitute a new category of sheet or strip steels, in terms of their high strength and enhanced formability. These excellent mechanical properties mainly arise from a martensitic transformation of metastable retained austenite, induced by external stress. The TRIP steels possess a multi-phase microstructure, consisting typically of ferrite, bainite and retained austenite. The microstructure is formed after intercritical annealing and a subsequent isothermal annealing in the bainitic transformation region, called austempering. The carbon content in austenite is enhanced both during the intercritical annealing and during the austempering. The carbon enrichment during austempering is the result of the suppression of the formation of carbides during the bainitic transformation, due to the presence of the alloying elements such as aluminium and silicon. The enrichment of carbon in the austenite increases its thermal stability and consequently, the austenite can be retained upon cooling to room temperature [1–5].

A quantitative determination of the volume fraction of the existing phases, especially the retained austenite, is essential for the evaluation of the TRIP steel properties. Experimental methods that have been reported in the literature include X-ray diffraction (XRD) [1–6], neutron diffraction [7], optical microscopy combined with image analysis [8], scanning electron microscopy (SEM) [9], Mössbauer spectroscopy [9,10], dilatometry [11], and magnetization measurements [12,13]. A summary of the characteristics of these techniques is presented in Table 1. Among them, the XRD method is the most frequently used as it is a suitable technique and XRD facilities are widely available. Other techniques are usually applied in order to overcome the

* Corresponding author. Tel.: +31-15-2782268; fax: +31-15-2786730.
E-mail address: l.zhao@tnw.tudelft.nl (L. Zhao).

0921-5093/01/$ - see front matter
PII: S0921-5093(01)00965-0

shortcomings of the XRD method. However, these methods have their own limitations with respect to the determination of the volume fraction of retained austenite in the TRIP steels with a multi-phase microstructure. For instance, the Mössbauer spectroscopy measurements require a very thin foil (20–50 μm), which leads to a different internal stress condition, in comparison to bulk samples. This may influence the results, since the retained austenite is very stress-sensitive. Dilatometry measurements make it possible to detect the fraction of transformed phase in-situ from the length change, but the measurement accuracy is not high since the knowledge of lattice parameters is limited and transformation plasticity may also affect the net dilatation. Magnetization measurements have intrinsic advantages as they are accurate and probe the bulk of the materials.

The present work aims to determine the volume fraction of retained austenite in TRIP steels by means of magnetization measurements. Furthermore, information with respect to the microstructure can be obtained from the approach to saturation and the demagnetizing factor of the magnetization curve. The reliability and accuracy of the measurements will be discussed, and compared with the results obtained from the XRD method.

Table 1
A comparison of the characteristics of different techniques for an analysis of the volume fraction of retained austenite

	Observed quantity	Probed volume	Accuracy
X-ray diffraction	Diffraction peaks	Surface layer	Normal
Neutron diffraction	Diffraction peaks	Bulk	Normal
Metallography/ SEM	Color-etched grain	Surface layer	Low
Mössbauer	Transmission spectra	Thin foil	High
Magnetization	Saturation magnetization	Bulk	High
Dilatometry	Length change	Bulk	Low

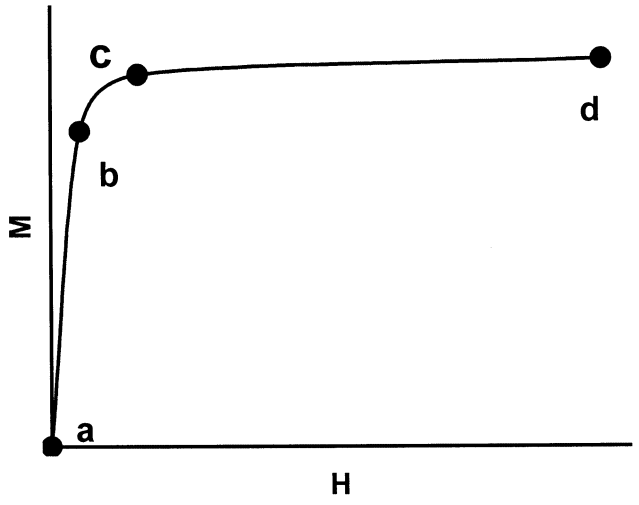

Fig. 1. Schematic illustration of the magnetization curve.

2. Background

Magnetic methods, such as magnetization measurements and thermo-magnetic analysis, are often used in metallurgical studies [13]. In magnetization measurements, the saturation magnetization can be obtained from the magnetization curve. The difference in saturation magnetization of specimens with and without austenite is directly related to the volume fraction of non-ferromagnetic retained austenite. This is due to the fact that ferrite, as well as martensite and cementite, is ferromagnetic at temperatures below the Curie temperature (for pure ferrite $T_C = 770°C$ and for cementite $T_C = 210°C$), while the austenite is paramagnetic [14].

The magnetization measurements give a relation between measured magnetization (M) and applied magnetic field (H), as schematically shown in Fig. 1. One can distinguish three different parts of the curve. In the first part, indicated by the line 'ab', the relation between M and H is almost linear. In this field region, the magnetic field inside the sample is reduced by the stray fields of the magnetized sample. The inverse of the initial slope is the so-called demagnetizing factor, which depends on the shape of the sample, on the volume fraction of the existing phases, as well as on their microstructure. In the case of a microstructure consisting of a continuous ferromagnetic matrix, in which inclusions of phases with different magnetic properties are embedded, the effective demagnetizing factor, N_{eff}, is estimated by [15,16],

$$N_{eff} = (1 - f)N_m + fN_p \quad (1)$$

where f is the volume fraction of the inclusions, for example, the retained austenite or the cementite. The so-called macroscopic demagnetizing factor, N_m, depends on the sample shape, and decreases with increasing the dimensional ratio (r) between the length and the width of the sample when the field is applied along the length of the sample. The microscopic demagnetizing factor, N_p, represents the shape anisotropy of the inclusions and their orientation distribution [13]. For instance, $N_p = 0$ if needle-like or plate-like inclusions are oriented with the long axis parallel to the magnetization direction. When the inclusions are randomly oriented, an average value of $N_p = 1/3$ is expected, independent of the shape. A deviation from $N_p = 1/3$ is, therefore, a sign of texture inside the sample, but not vice versa, because $N_p = 1/3$ when the shape of the inclusions is spherical.

Table 2
Chemical composition (wt.%) of the TRIP steels Al1.8 and Al1.4P[a]

Code	C	Mn	Al	Si	P	N	Ac_1	Ac_3
Al1.8	0.20	1.53	1.8	0.02	<0.005	0.004	761	1037
Al1.4P	0.18	1.52	1.4	0.02	0.081	0.0055	747	1017

[a] The starting and finishing temperatures of the ferrite to austentie transformation, Ac_1 and Ac_3 (°C), have been determined by dilatometry experiments [21].

The second part of the curve, indicated by 'bc' in Fig. 1, is the transition region characterized by domain wall movements and the reorientation of spins following the domain wall movement. The characteristics of the transition thus depend on the existing preferred orientation (texture). The approach to saturation, shown as the line 'cd' in Fig. 1, is used for the determination of the volume fraction of retained austenite. In this region, a rather large increase in H is required to produce a relatively small increase in M. This behavior is associated with microstructural effects, and depends on rotations and reorientation of spins. The approach to saturation is usually described by [13,17]

$$M = M_s\left(1 - \frac{a}{H} - \frac{b}{H^2}\right) \quad (2)$$

where M_s is the saturation magnetization. The parameters a (in A m^{-1}) and b (in A^2 m^{-2}) are positive constants, which can be ascribed to different physical origins. Parameter a arises from nano-scale microstructural effects such as inclusions, voids, point defect and/or microstresses, and parameter b from the crystal anisotropy.

The volume fraction of retained austenite, f_γ, can be determined by a comparison of the M_s values in the austenite-containing sample, $M_s(c)$, and in the austenite-free sample $M_s(f)$,

$$f_\gamma = \frac{M_s^a - M_s(c)}{M_s^a} = 1 - \beta\frac{M_s(c)}{M_s(f)} \quad (3)$$

where $\beta = M_s(f)/M_s^a$ is the ratio between the saturation magnetization of the austenite-free sample and that of ferrite (M_s^a). The austenite-free sample contains besides ferrite also a small volume fraction of cementite, which can be estimated from the composition of the materials using the lever-rule. The coefficient β thus can be obtained from the published data of the saturation magnetization of the ferrite ($M_s^a = 1.714 \times 10^6$ A m^{-1} [13] for pure iron) and cementite ($M_s^\theta = 0.99 \times 10^6$ A m^{-1} [18,19]) via the relation $\beta = 1 - f_\theta + f_\theta$ $[M_s^\theta/M_s^a]$. In the derivation of Eq. (3), it is assumed that the amount of cementite precipitates is negligible after austempering of the TRIP steels, since the addition of alloying elements such as aluminium significantly suppresses the formation of cementite during the bainitic transformation [1–5].

3. Experimental

The two aluminium containing TRIP steels examined in this investigation were produced via hot rolling and air cooling, and had an as-received thickness of 6 mm. The composition of the materials is shown in Table 2. The materials were machined to cylinders with a diameter of 5 mm and a length of 10 mm for heat treatments under vacuum in an 805a type Bähr dilatometer. In order to design the appropriate thermal schedules, the transformation temperature (Ac_1 and Ac_3) were determined by dilatometry. The results are listed in Table 2. The samples were pre-annealed for 10 min at 900°C, which is in the two-phase region, and then quenched at 25°C s^{-1} to 400°C, held at this temperature for 0, 0.5, 1.0, 1.5, 2.0, 3.0, 5.0 and 10.0 min, respectively, and subsequently cooled at approximately 2°C s^{-1} to room temperature.

The magnetization measurements were performed in a Quantum Design SQUID magnetometer (MPMS-5S). In SQUID magnetization measurements, an applied magnetic field is used to induce a magnetization in the sample. The sample magnetization produces stray fields, which are subsequently probed up to a very high accuracy by a superconducting SQUID device. The equipment is calibrated periodically with standard nickel and palladium spheres (with a sensitivity of 1×10^{-11} A·m^2). During the measurement of the cylindrical sample, the magnetic field was applied to a maximum value of 5 T ($H = 3.98 \times 10^6$ A m^{-1}) and then decreased stepwise to zero field, i.e. from 5 to 0.25 T in steps of 0.25 T, from 0.25 to 0 T in steps of 0.05 T. The measurements were performed in decreasing field in order to create a well-defined field history for the magnetization. The measuring temperature was regulated at 26.85 ± 0.05°C. The relative error of the measured data is smaller than 0.5%. As-received material was considered to be austenite-free, which was confirmed by XRD measurements. In order to fit the approach to the saturation of the measured magnetization data and the physically significant parameters described in Eq. (2), a linear least-squares fitting of the 'cd' line in Fig. 1 is applied, and the fitting error is obtained from the standard definition [20].

After the magnetization measurements, disks with a diameter of 5 mm were cut along the transverse direc-

tion of the cylinder samples and polished for the XRD measurements. Very low force was applied during cutting and mechanical polishing in order to avoid stress-induced transformation of the retained austentie. The XRD measurements were performed on a Siemens' X-ray diffractometer using CoKα radiation. A more detailed description of experimental conditions and results of the XRD measurements has been published elsewhere [21].

4. Results

4.1. Volume fraction of retained austenite

The magnetization as a function of the applied magnetic field was measured for both compositions and all

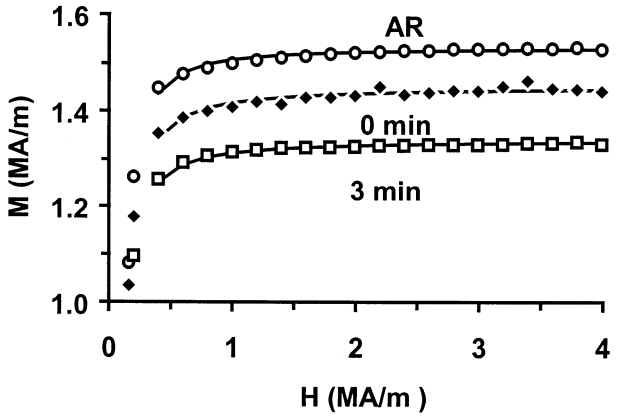

Fig. 2. Measured magnetization as a function of the applied magnetic field for Al1.8 samples. The open circles represent the as-received (AR) sample, the solid diamonds the sample without austempering (0 min), and open squares the sample with austempering at 400°C for 3 min. the lines correspond to fits with Eq. (2).

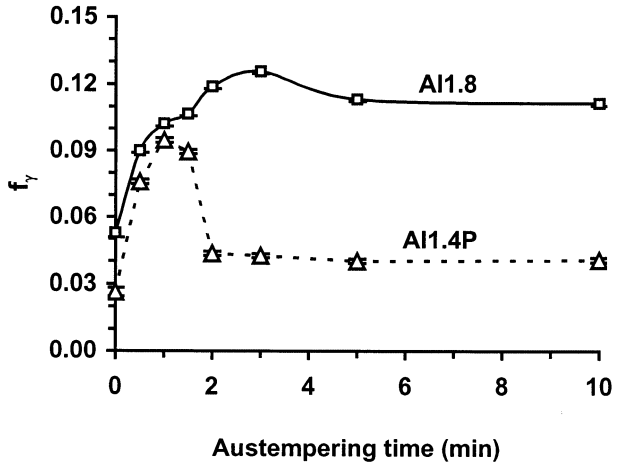

Fig. 3. The volume fraction of retained austenite f_γ as a function of austempering time. The experimental error is smaller than the symbol size.

austempering times applied. Three representative magnetization curves at $H \geq 0.2 \times 10^6$ A m^{-1} and the fits to Eq. (2) are shown in Fig. 2. From the fits, the saturation magnetization M_s was obtained with a relative error less than 0.2%. It was found that the M_s values in the as-received steels (1.533×10^6 A m^{-1} for the Al1.8 sample and 1.475×10^6 A m^{-1} for the Al1.4P sample) were about 11 and 14% smaller than the M_s of pure iron, which is 1.714×10^6 A m^{-1} [13]. This is due to the presence of cementite with a lower M_s, (leading to a decrease of around 1%) and the addition of alloying elements including carbon, manganese, aluminium, phosphorous and silicon in the TRIP steels, as well as the sample size effect. Taking the dependence of M_s on composition as reported in literature [18,22] and assuming no partitioning of the alloying elements, a decrease of M_s of 7.2 and 6.2% is calculated for both steel grades. Nevertheless, since M_s for the Al1.8 sample is larger than the one for the Al1.4P sample, the decrease in M_s is not simply proportional to the amount of aluminium, which is the main difference in composition for these two steels. The effect of the third factor leading to a decrease of the experimental value of M_s, viz. the relatively large sample size, was investigated by measurements on cylindrical samples of 1 mm in diameter and 2 mm in length. It was found that the M_s values in the small samples were approximately 3% larger than those obtained from the large samples. However, the sum of these three effects (11% for the Al1.8 and 10% for the Al1.4P sample) is still lower than the measured decrease of the M_s value for the Al1.4P sample. This may be due to non-linear effects as the alloys contain a combination of different elements.

The volume fraction of the retained austenite is calculated from the saturation magnetization, M_s, using Eq. (3). The coefficient $\beta = M_s(c)/M_s^a$ is estimated to be 0.987 for the Al1.8 sample and 0.989 for the Al1.4P sample, based on the chemical composition of the materials in Table 2 and the published M_s values for ferrite and cementite. It is interesting to note that the value of β is insensitive to variations in M_s^a caused by alloying elements as they affect $M_s(f)$ in a similar way for small concentrations. This is also true for the evaluation of the fraction of retained austenite determined by Eq. (3) as the alloying concentrations are equal in the TRIP samples and the austenite-free sample.

Fig. 3 shows the calculated fraction as a function of the austempering time in the Al1.8 and Al1.4P samples. One can see that the fitting errors are nearly negligible, since the standard deviation (S.D.) is 0.002, indicating that the measured data are accurate with respect to the determination of the volume fraction of retained austenite, even though some deviations in the magnetization curve are observed. It is noteworthy that similar results, but with lower accuracy, are obtained when the magnetization at the maximum applied magnetic field is used instead of M_s in Eq. (3).

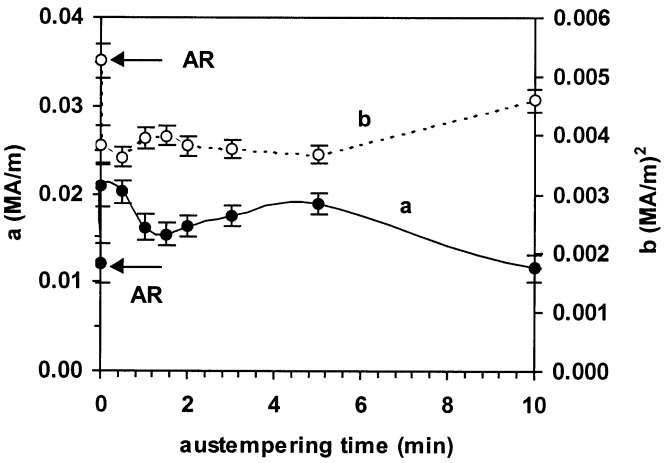

Fig. 4. Parameters a and b as a function of the austempering time at 400°C for the Al1.8 samples. 'AR' stands for the as-received sample.

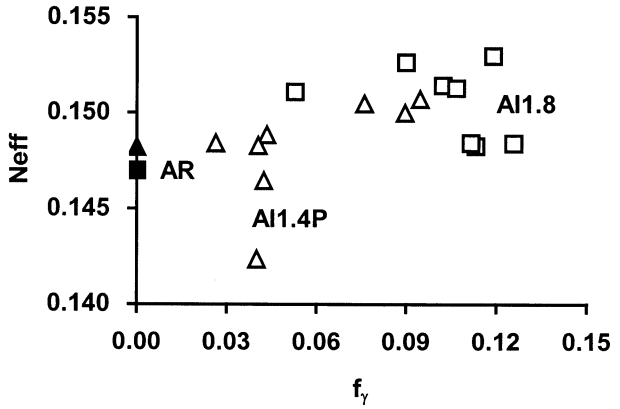

Fig. 5. The effective demagnetizing factor N_{eff} as a function of volume fraction of retained austenite f_γ in Al1.8 and Al1.4P samples.

The dependence of the volume fraction on the austempering time reveals valuable information regarding the transformation behavior in the two steels. About 5.6 and 2.5% of austenite are retained in the as-quenched (austempering time zero) Al1.8 and Al1.4P samples, respectively. In the first stage of austempering, the volume fraction retained austenite increases with increasing austempering time, and reaches a maximum value. This indicates that more austenite is retained as a result of its increased stability due to the increased carbon concentration. The carbon enrichment arises from the suppression of carbide formation during the bainitic transformation. For the annealing time leading to the maximum in retained austenite, the carbon enrichment moves the martensite starting temperature of the austenite to a temperature below room temperature. For longer annealing times, the fraction decreases, gradually for the Al1.8 samples and more rapidly for the Al1.4P samples. The martensite starting temperature is still below room temperature, but the fraction of retained austenite decreases as the bainitic transformation continues. One can also see that a higher aluminium concentration leads to a higher fraction of retained austenite. A higher aluminium concentration also increases the holding time required to obtain the maximum. These two trends may be related to each other, and are attributed to the increased suppression of carbide formation with increasing aluminium concentration.

4.2. Relation between the $M-H$ curve and the microstructure

In addition to providing the M_s value, the magnetization measurements can also reveal information on the microstructure. From the fitting procedure, one obtains the microstructure related parameters, a and b, as described in Eq. (2). Fig. 4 shows the variation of these parameters during austempering and the errors resulting from the fitting procedure for the Al1.8 samples.

Although the strong mathematical correlation between the two parameters affects the values obtained, it may be concluded that the absolute values of b/H^2 are always smaller than those for a/H in the relevant range for H. This indicates that domain rotation is more influenced by nano-scale microstructural aspects, such as voids, inclusions, point defects and microstresses, than by the crystal anisotropy. The difference between a/H and b/H^2 is smaller in the as-received than in the as-quenched samples. This might be due to the decrease in microstress and the fraction of inclusions as a result of intercritical annealing. The difference between a/H and b/H^2 increases during the bainitic transformation before the maximum volume fraction, showing the increase of microstress, and possibly the inclusions, resulting from the phase transformation.

In the low magnetic field range of the magnetization, indicated by the 'ab' line in Fig. 1, the observed magnetization can be related to the presence of demagnetization fields. The effective demagnetizing factor, N_{eff}, is deduced from the inverse slope of the $M-H$ curve in low magnetic fields, as a function of the volume fraction of retained austenite, and the results are shown in Fig. 5. As can be seen, all demagnetizing factors range between 0.140 and 0.155. In the present cylindrical samples with a height of 10 mm, a diameter of 5 mm and a high permeability ($10^2 \sim 10^3$ μ_o [13]), a geometrical demagnetizing factor, N_m, of 0.14 [13,18] is expected for a sample, which is homogeneously magnetized along the cylindrical axis. Further analysis of published data [13] reveals that the derivative of the geometrical demagnetizing factor with respect to the dimensional ratio r is $dN_m/dr = -0.075$ in the vicinity of $r = 2$. This indicates that the shape differences in the samples due to the limited accuracy of machining or due to the phase transformations during the heat treatment procedure [23] have a negligible effect on N_m with respect to the measured demagnetizing factor.

The difference between the N_{eff} and N_m values can be understood from Eq. (1). The microscopic demagnetizing factor, N_p, reflecting the average texture and the shape anisotropy of the inclusions, is thus calculated. The results are shown in Fig. 6. The values for the as-received samples where $f_\gamma = 0$ were calculated by assuming that the fraction of cementite is 3% and it can be treated as an inclusion as since it possesses a lower magnetization in comparison to the ferritic matrix. The N_p values for the as-received samples are between 0.35 and 0.45. After austempering, the N_p values generally decrease as the volume fraction of retained austenite increases. The influence of texture can be seen from the deviation of the N_p values from the value 1/3. This might be due to the fact that part of the retained austenite is present along grain boundaries. Nevertheless, since the magnetization shows a complex relation to the microstructure, the parameters (N_p, a and b) derived from the magnetization curve only give a qualitative description of the microstructure. To characterize the microstructure in more detail, it is recommended to combine this magnetic technique with other techniques.

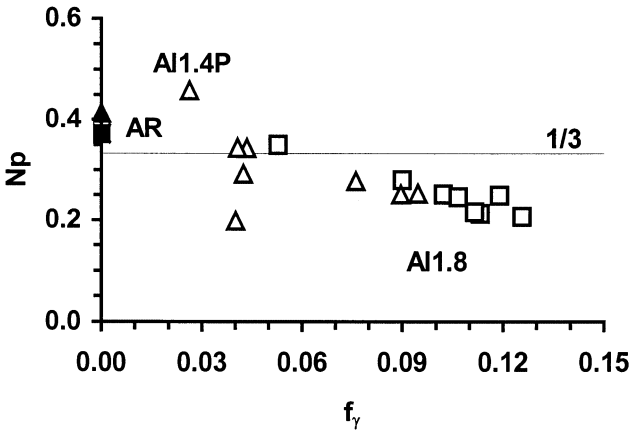

Fig. 6. The microscopic demagnetizing factor N_p as a function of the volume fraction of retained austenite f_γ in Al1.8 (squares) and Al1.4P (triangles) samples. 'AR' stands for the as-received sample.

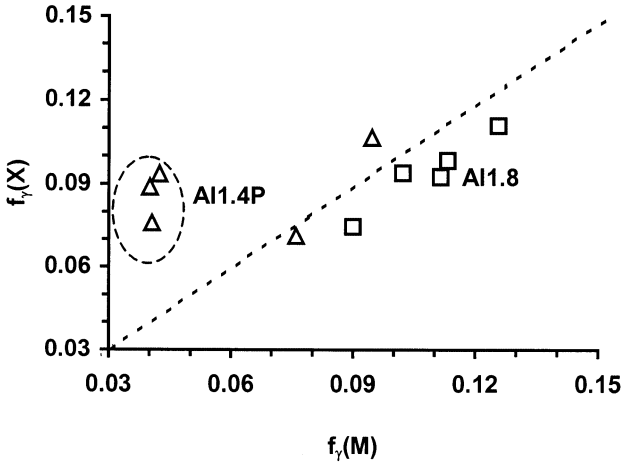

Fig. 7. A comparison of the volume fractions of retained austenite in Al1.8 (squares) and Al1.4P (triangles) samples, determined by magnetization measurements (f_γ(M)) and X-ray diffraction measurements (f_γ(X)).

5. Discussion

From the magnetization curves, the volume fraction of retained austenite in TRIP steels and other information concerning the microstructure can be derived. The fraction was obtained from the fitted M_s value. The error resulting from the fitting procedure appears to be very small. However, to understand the results better, the following three aspects should be kept in mind. Firstly, the fraction of retained austenite as defined by Eq. (3) is based on three assumptions, namely (a) the value of β, (b) the as-received samples are free of austenite, and (c) there is no carbide formation during the bainitic transformation. These assumptions are unlikely to lead to large errors, but need to be examined in more detail if higher accuracy were required. Secondly, the effect of sample size might be taken into account. The length of the present samples is close to the upper limit of the instrumental capabilities. This can cause a systematic error, which would not influence the results for the volume fraction being a relative ratio of the M_s values, but would influence the analysis of the microstructure related parameters including the demagnetizing factors N_p and N_{eff}. This can be improved by using a smaller sample with a higher dimensional ratio for a better analysis of the 'cd' line in Fig. 1, or with a lower dimensional ratio for the 'ab' line. Thirdly, the magnetization measurements also detect all other non-ferromagnetic phases besides retained austenite. However, this influence is not likely to be significant in the present case.

To put the results obtained with the magnetization methods in a wider perspective, the volume fractions are compared with those obtained by XRD measurements. XRD is currently the most widely applied technique for the determination of the volume fraction of retained austenite [6]. The XRD measurements were performed on the same samples and have been published elsewhere [21]. The development of the volume fraction of retained austenite as a function of the austempering time is similar to the one in Fig. 3, viz, a maximum fraction is found at a specific austempering time and a higher aluminium concentration leads to a higher fraction in most cases. From Fig. 7, the volume fractions of retained austenite in Al1.8 and Al1.4P samples as determined from magnetization and the XRD measurements can be compared. As can be seen, the absolute values of the volume fractions do not coincide, the volume fractions in the Al1.8 samples

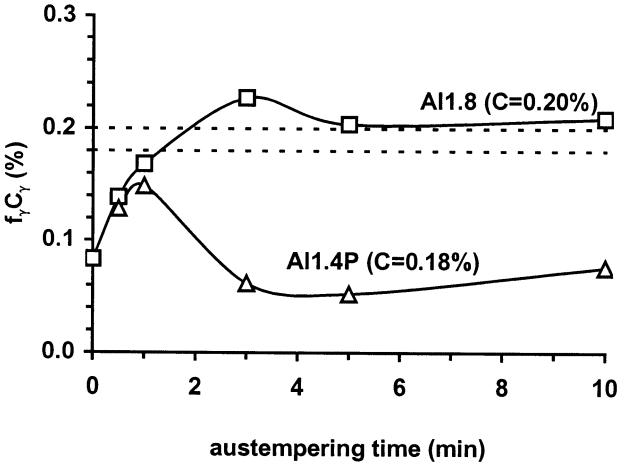

Fig. 8. The product of the carbon concentration obtained from the XRD measurements and the volume fraction of retained austenite from the magnetization measurements as a function of austempering time in the Al1.8 and Al1.4P samples. The two dashed lines represent the total carbon concentration in the two materials.

from magnetization measurements are slightly larger than the ones from the XRD. On the other hand, the austenite fractions in the Al1.4P samples from magnetization measurements are in general smaller than the ones from the XRD. The difference is particularly obvious for the three data points indicated in the figure, which correspond to holding times longer than the time to reach the maximum fraction.

These results are further analyzed by combining the volume fraction f_γ and the carbon concentration C_γ in retained austenite, where the fraction was determined from the magnetization measurements and carbon concentration from the peak position in the XRD profiles [21]. The product of these two values $f_\gamma C_\gamma$ is the amount of carbon retained in the austenite and is often regarded as a measure for the TRIP effect. In Fig. 8, the product $f_\gamma C_\gamma$ is plotted as a function of austempering time in the two steels. In the Al1.8 samples, the product increases as a result of the bainitic transformation. Almost all carbon in the steel is contained in the retained austenite after austempering for 2 min, reflecting the strong effect of aluminium on the suppression of carbide formation. However, the amount of carbon in the retained austenite in the Al1.4P samples decreases rapidly after its maximum (the decrease is slower but still significant if the fractions deduced from the XRD measurements were used). The difference in behavior possibility suggests a different mechanism concerning the partitioning of carbon in retained austenite, which is a subject for further study. The results suggests that a more controlled austempering procedure is required for the Al1.4P material, due to its sensitivity to the austempering time, as compared with the Al1.8 material. It is noteworthy that some authors [6] commented that the determination of the carbon concentration by the XRD method is less accurate than that of the volume fraction. This is due to lack of a reliable relation between the carbon concentration and the lattice parameter of austenite for the TRIP steels. This is a possible reason why the amount of carbon in the retained austenite even slightly exceeds the total amount of carbon in the Al1.8 samples, as shown in Fig. 8.

The discrepancy in the measured volume fractions from the XRD measurements and the magnetization measurements can be considered against possible experimental errors occurring in the XRD method. These errors may arise from the sample condition, the instrumental limitation and the calculation method. Detailed factors include surface, texture, grain size, step size of scanning, focussing, statistical counting, peak boundary, R-values, etc. In this particular case, the following factors are likely to result in significant errors (a) the stress condition on the sample surface alters the diffraction signals from the retained austenite, and consequently influences the calculated volume fraction, as well as the carbon concentration; (b) errors may arise from the particular equation used to calculated the fraction, the number of diffracted peaks and the calculation of the theoretical intensity (R-values) [6,24], in which the R-values are usually calculated without considering the strong change in the carbon concentration in austenite during austempering; (c) it is difficult to take into account the effect of texture on the integrated intensity of the diffracted peaks, especially in cases when the type and strength of texture in retained austenite, ferrite and bainitic ferrite are different; (d) the integrated intensity of the small austenite peaks is very sensitive to the procedures to determine the background and peak boundaries.

It is hard to quantify the total error in the XRD measurements caused by the above factors. If one compares the relevant factors in the XRD measurements and the magnetization measurements qualitatively, the factors from the XRD measurements are more difficult to control. Therefore, it is suggested that the fractions from the magnetization measurements are more reliable than the ones from the XRD. Moreover, the XRD measurements are incapable of detecting the retained austenite in the as-quenched samples, since a high internal stress results in a broadening of the diffracted peaks. This means that the magnetization measurements are capable to detect small amounts of retained austenite. It is, therefore, concluded that magnetization measurements are a more effective technique to determine the volume fraction of retained austenite in TRIP steels, although it has the intrinsic limitation that it does not give information on the carbon concentration in retained austenite.

6. Conclusions

In this work the volume fraction of retained austenite in two aluminium-containing TRIP steels was investigated by magnetization and X-ray measurement. It was found that the fraction of retained austenite as a function of the austempering time shows a clear maximum. The rate of decrease is stronger for the Al1.4P material than for the Al1.8 material. This indicates that the Al1.4P material is more sensitive to austempering time than the Al1.8 material. Moreover, additional information with respect to the microstructure was obtained from the magnetization curves as a function of the applied magnetic field. It seems that magnetization measurements lead to a more reliable and more sensitive detection of the retained austenite than X-ray measurements.

Acknowledgements

The authors gratefully acknowledge Dr H.G.M. Duijn, van der Waals — Zeeman Institute, University of Amsterdam, for his assistance with the magnetization measurements, Dr R. Delhez and Ing. N.M. van der Pers, Laboratory for Materials Science, Delft University of Technology, for their assistance in the XRD measurements and fruitful discussions. Also, we would like to thank Dr J. Vrieze and M.A. de Haas, Corus Research & Development, IJmuiden, The Netherlands, for their continuous interest in the subject studies.

References

[1] H.C. Chen, H. Era, M. Shimizu, Metall. Trans. 20A (1989) 437.
[2] W.C. Jeong, D.K. Matlock, G. Krauss, Mater. Sci. Eng. A165 (1993) 9.
[3] O. Matsumura, Y. Sakuma, H. Takechi, Trans. ISIJ 32 (9) (1992) 1014.
[4] A. Itami, M. Takahashi, K. Ushioda, Proceedings of the International Symposium on Low-Carbon Steels of the 90', Pittsburgh, October 1994, pp. 245.
[5] K. Sugimoto, N. Usui, M. Kobayashi, S. Hashimoto, ISIJ Int. 32 (1992) 1311.
[6] M. de Meyer, D. Vanderschueren, K. de Blauwe, B.C. de Cooman, The 41st MWSP Conference Proceedings, vol. XXXVII, 1999, pp. 483.
[7] M. Bouet, J. Root, E. Es-Sadiqi, S. Yue, Mater. Sci. Forum 284–286 (1998) 319.
[8] A. Basuki, E. Aernoudt, Scr. Mater. 40 (1999) 1003.
[9] P. Jacques, X. Cornet, P. Harlet, J. Ladrière, F. Delannay, Metall. Mater. Trans. 29A (1998) 2383.
[10] J.H. Ladrière, X.J. He, Mater. Sci. Eng. 77 (1986) 133.
[11] A. Ali, M. Ahmed, F.H. Hashimi, A.Q. Khan, Metall. Trans. 24A (1993) 2145.
[12] W. Bleck, K. Hulka, K. Papamentellos, Mater. Sci. Forum 284–286 (1998) 327.
[13] J.W. Cahn, P. Haasen, Physcial Metallurgy, Third ed, Elsevier, Amsterdam, 1983, p. 2558.
[14] B.D. Cullity, Introduction to Magnetic Materials, Addison-Wesley, Reading, MA, 1972.
[15] J. Dubowik, Phy. Rev. 54B (2) (1996) 1088.
[16] Y.G. Pogorelov, G.N. Kakazei, M.M.P. de Azevedo, J.B. Sousa, J. Magn. Magn. Mater. 196–197 (1999) 112.
[17] J.E. Goldman, A. Arrott, Magnetic Properties of Metals and Alloys, ASM, Cleveland, Ohio, 1959.
[18] R.M. Bozorth, Ferromagnetism, D. van Nostrad Company Inc, New York, 1961, p. 367.
[19] F.C. Schweer, C.E. Spangler, J.F. Kelly Jr, Acta Metall. 26 (1978) 579.
[20] J.R. Green, D. Margerison, Statistical Treatment of Experimental Data, Elsevier, Amsterdam, 1978.
[21] L. Zhao, J. Sietsma, S. van der Zwaag, in: P. Neumann, et al. (Eds.), Steels and Materials for Power Plants, vol. 7, Wiley, Weinheim, 2000, p. 77.
[22] A.E. Berkowitz, E. Kneller, Magnetism and Metallurgy, Academic Press, New York, 1969, p. 294.
[23] C. Qiu, S. van der Zwaag, Steel Res. 88 (1) (1997) 32.
[24] C.F. Jatczak, J.A. Larson, S.W. Shin, Retained Austenite and its Measurements by X-ray Diffraction, Society of Automotive Engineers, Inc, Warrendale, PA, 1980.